

Investigation of the Rheological Behavior of Titanium Dioxide Pigmented Acrylonitrile–Butadiene–Styrene Polymer

Soheil Farshbaf Taghinejad,¹ Mina Behrouzi,² Saeed Asiaban²

¹Iran Petrochemical and Polymer Institute, Tehran, Iran

²National Petrochemical Co., Research and Technology Co., Tehran, Iran

Received 30 June 2010; accepted 9 July 2011

DOI 10.1002/app.35225

Published online 25 October 2011 in Wiley Online Library (wileyonlinelibrary.com).

ABSTRACT: Titanium dioxide (TiO₂) pigments may be surface-modified by hydrous oxides, such as alumina (e.g., Cristal 134) or by organic compounds, such as organophosphate (e.g., Tiona 188). In this investigation, the effects of these pigments on the rheological properties of acrylonitrile–butadiene–styrene (ABS) polymer were investigated. With the oscillatory rheometry method in the linear viscoelastic region, the storage and loss moduli versus frequency graph of ABS in the molten state showed two crossover points (COPs) when the surface of the ABS components, that is, poly(styrene-*stat*-acrylonitrile) and poly[(styrene-*stat*-acrylonitrile)-*graft*-polybutadiene] or *g*-ABS, had good interaction. The first COPs increased when the TiO₂ content rose to 0.5 and 1.5% in Tiona 188 and Cristal 134 pigmented ABS samples, respectively. With the addition of TiO₂ up to these contents, the polymer-pig-

ment interaction becomes stronger so that the dispersion of the pigments was good. With increasing TiO₂, the first COPs dramatically decreased because of agglomeration of the pigments. The shifting of the first COP may be applied as a criterion to specify the dispersion of TiO₂ particles in the ABS matrix. Scanning electron micrographs showed that the pigments had no effect on the size of the polybutadiene particles. Also, transmission electron micrographs proved that agglomerates of Tiona 188 and Cristal 134 particles were formed above 0.5 and 1.5% TiO₂ contents, respectively. © 2011 Wiley Periodicals, Inc. *J Appl Polym Sci* 124: 2016–2021, 2012

Key words: compounding; dyes/pigments; plastics; polymer rheology; surface modification

INTRODUCTION

Acrylonitrile–butadiene–styrene (ABS) polymer is a terpolymer that has many applications in automotive and household industries. To improve its physical and mechanical properties, ABS is blended with fillers, such as calcium carbonate and talc. Also, titanium dioxide (TiO₂) pigment can be used to increase the whiteness and opacity and decrease the yellowness of ABS parts. Although these materials have some beneficial effects for ABS polymer, they may cause some unfavorable effects in ABS parts, so it is necessary to investigate the effects of these materials on ABS properties.

We investigated the effects of the surface treatment type and content of TiO₂ pigment on the optical aspects and physical and mechanical characteristics, including the tensile strength, Izod impact strength, and Rockwell hardness of a general-pur-

pose ABS polymer.¹ Treating the surface of the TiO₂ pigments improved their weather resistance and dispersability. TiO₂ pigments may be surface modified by hydrous oxides, such as alumina (e.g., Cristal 134) or by organic coatings, such as organophosphates (e.g., Tiona 188). In this study, we intended to investigate the effects of both of these pigments on the rheological properties of a general-purpose ABS polymer.

Because of the correlation between the rheology and morphology of polymer blends and composites, the rheological properties were examined to determine the morphology of neat ABS and its blends and composites.

Aoki and Nakayama^{2–5} and Bertin et al.⁶ investigated the effects of ABS microstructural parameters, such as the content and particle size of poly(styrene-*stat*-acrylonitrile) (SAN), and also the grafting degree of dispersed polybutadiene rubber and the molecular weight of the components, on the ABS rheological properties. By means of an oscillatory deformation rheometry method, they studied the rheological behavior of different ABS resins so that existence of a solidlike behavior of molten ABS at low frequencies was indicated. However, this phenomenon occurred in a specific range of contents and SAN grafting of dispersed butadiene rubber (BR).

Correspondence to: S. Asiaban, F5 Building, Iran Petrochemical and Polymer Research Institute, Pajooresh Boulevard, P. O. Box 1497713115, Tehran-Karaj Highway, Tehran, Iran (s.asiaban@npc-rt.ir).

TABLE I
Composition¹² of ABS Manufactured by Tabriz Petrochemical Co.

| | | | |
|-------|-------------|---------|---------------|
| SAN | Component | Styrene | Acrylonitrile |
| | Content (%) | 56.19 | 43.81 |
| g-ABS | Component | SAN | Butadiene |
| | Content (%) | 39.9 | 60.1 |

Takahashi et al.⁷ and Li et al.⁸ studied the nonlinear and elongation flow behaviors of ABS, respectively. In addition, the effects of rigid inorganic particles, such as CaCO₃,⁹ nanometer CaCO₃,¹⁰ and nanosilica,¹¹ on the rheological properties of ABS have been investigated.

EXPERIMENTAL

Materials

SAN and poly[(styrene-*stat*-acrylonitrile)-*graft*-polybutadiene] (*g*-ABS) were supplied from Tabriz Petrochemical Co. (Tabriz, Iran). The specifications of the used SAN and *g*-ABS are shown in Table I.¹²

Alumina-surface-treated TiO₂ (Cristal 134) and organophosphate-surface-treated TiO₂ (Tiona 188) were supplied from Cristal Co., (Jeddah, Saudi Arabia). In both of the TiO₂ pigments, the content of surface-treated material was about 2%, so the content of TiO₂ in both pigments was almost the same.

Sample preparation

First, SAN and *g*-ABS were dry-blended with a 3 : 2 weight ratio. Then, TiO₂ pigments were added to the mixture at 0.2, 0.5, 1.5, 3, 6, 10, and 20%. The samples containing Cristal 134 and Tiona 188 were named C2, C5, C15, C30, C60, C100, and C200 and T2, T5, T15, T30, T60, T100, and T200, respectively. Each sample was melt-blended with an extrusion process in a ZSK25 twin-screw corotating compounder (Coperion Co., Stuttgart, Germany). The screw speed and feeding rate were 550 rpm and 8 kg/h, respectively. The heating-zone temperatures were fixed at 180, 190, 200, 210, 215, and 220°C.

After compounding, each sample was molded with a compression-molding process at 25 MPa and 205°C to prepare sheets for rheological measurements, scanning electron microscopy (SEM), and transmission electron microscopy (TEM) analyses.

Rheological measurements

Rheological measurements were performed with Anthon Paar MCR-300 rheometer (Osterreich, Austria). All rheometry tests were performed under a nitrogen atmosphere. Strain sweep tests were performed to determine the linear viscoelastic region.

The strain amplitude for all samples was fixed at 1%, and the test temperature was 220°C.

SEM

SEM images were taken with a VEGA\TESCAN scanning electron microscope (Tescan Co., Brno, Czech Republic). SEM images were taken of the fracture surfaces of ABS sheets that were broken under liquid nitrogen.

TEM

The TEM examination was conducted with a transmission electron microscope (EM 208S Philips, Eindhoven, The Netherlands) operating at 100 kV. According to the recommended procedure, the samples were prepared from the specimens with an ultramicrotome equipped with a diamond knife.

RESULTS AND DISCUSSION

For almost all of the molten homopolymers, the oscillatory-mode rheological properties in a wide range of frequencies were the same. Figure 1 illustrates this behavior. In the low-frequency region (terminal region), terminal behavior could be seen. In this region, the loss modulus (G'') was greater than the storage modulus (G'). Also, G'' and G' were proportional to ω (frequency) and ω^2 , respectively.¹³

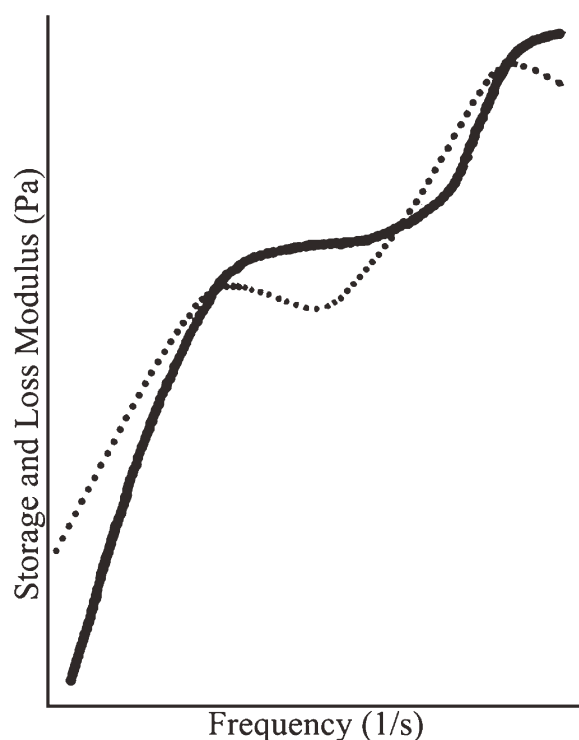


Figure 1 G'' and G' of the homopolymers.

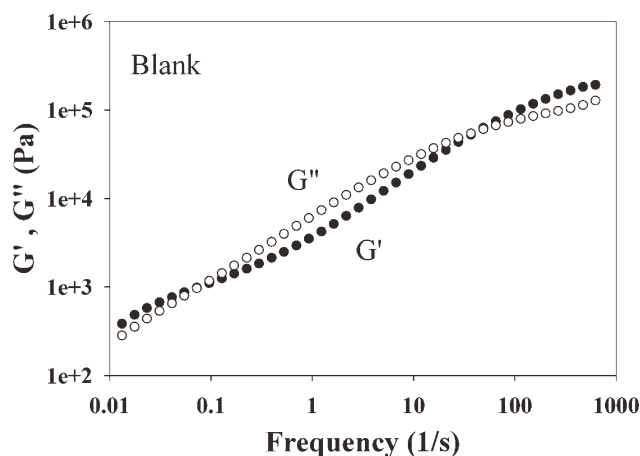


Figure 2 Nonterminal behavior of neat ABS (blank sample).

It should be noted that sharp curves in Figure 1 could be seen in polymers with a narrow distribution molecular weight.¹⁴

ABS polymer is not a homopolymer because it is a core-shell secondary blend in which the SAN matrix includes core-shell particles of *g*-ABS. In the low- ω region, ABS showed nonterminal behavior in specific microstructure conditions;²⁻⁶ also, the G'' and G' curves met together and made two crossover points (COPs). The first COP occurred at low frequencies, and the second COP occurred at high frequencies. The formation of the first COP was due to the strong interaction of the matrix and disperse phases and the longer relaxation time of butadiene compared to SAN. This behavior created an elliptical area where $G'' > G'$. As Figure 2 shows, the broadness of this area was related to the viscous behavior of the melt in the terminal region.

With the addition of TiO_2 pigment, the first COP shifted to higher frequencies, G' increased, and the elliptical area decreased. The molten composites containing Cristal 134 pigment had more elasticity, and the first COPs shifted to higher frequencies in comparison with the Tiona 188 related samples. This behavior is shown for the C5 and T5 samples in Figure 3. The surface of the Cristal 134 pigment was treated by a hydrous oxide, that is, alumina. Therefore, it had better interaction with the polar matrix (SAN) and better dispersion so that the Cristal 134 pigment made a stronger physical network than Tiona 188. On the other side, organophosphate chains on the surface of Tiona 188 caused the pigment particles to strongly stick together. Therefore, the diffusion of the SAN matrix chains into the pigment aggregates became so difficult¹⁵ so that polymer-pigment interaction was weak and also the pigment was not well dispersed.

In Figure 4, the first COP frequency versus the TiO_2 content (ϕ_T) is plotted for Cristal 134 and Tiona

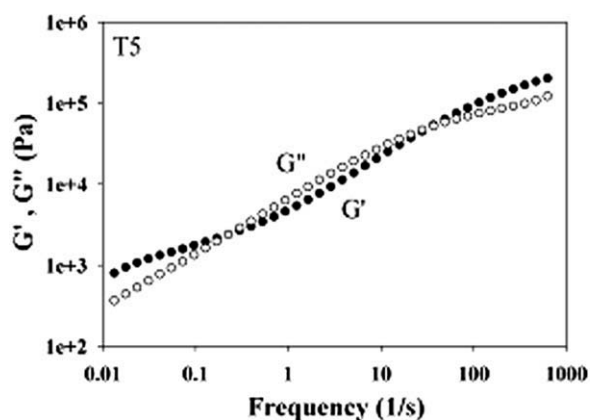
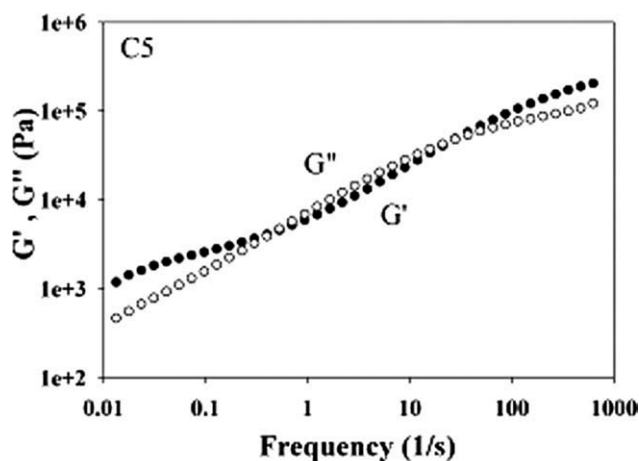


Figure 3 G'' and G' for the C5 and T5 samples at 220°C.

188 pigmented ABS. The first COPs increased when ϕ_T increased up to 0.5 and 1.5% in the Tiona 188 and Cristal 134 pigmented ABS polymers, respectively. In other words, with the addition of TiO_2 up to these percentages, the polymer-pigment interaction became stronger, so the dispersion of the pigments was good. Also, because of the better

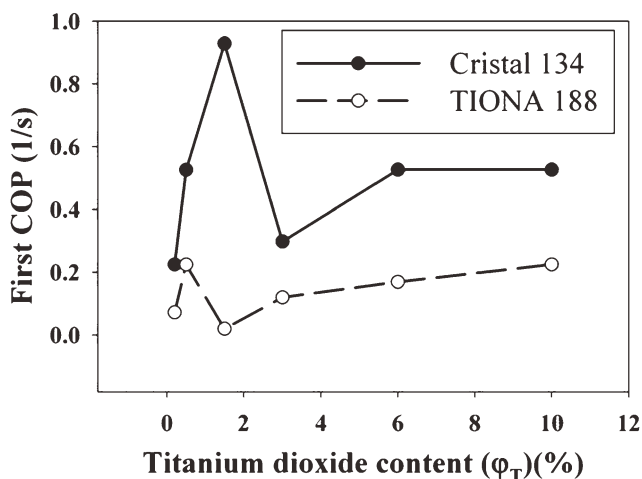


Figure 4 First COP variation in ABS contained Cristal 134 and Tiona 188.

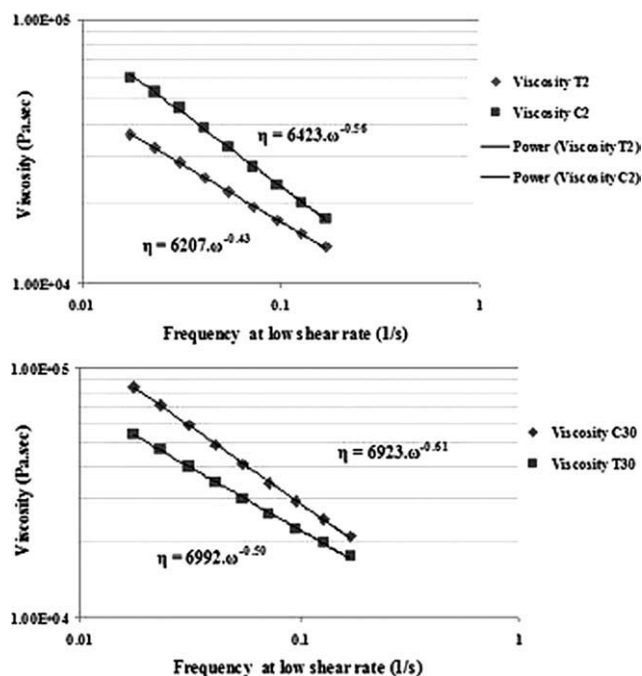


Figure 5 Complex viscosity (η) versus ω at low- ω region.

dispersion of Cristal 134, the maximum first COP occurred at higher ϕ_T . After the maximum points, with increasing TiO₂, the first COPs dramatically decreased because of the agglomeration of the pigments and the decrease in their surface area. The Cristal 134 related COP was always higher than the Tiona 188 related COP.

Remarkably, the aforementioned results agreed with the results of a previous author's research.¹ The increases in the content of organic and inorganic surface-treated TiO₂ pigments up to 0.5 and 1.5%, respectively, caused an increase in the impact strength and a decrease in the yield stress of the pigmented ABS samples because of the good dispersion of the pigments and suitable interparticle spacing. In other word, under these contents of TiO₂ pigment, the particles were well dispersed so that stress concentration on the particles was homogeneously distributed; eventually, this caused the matrix to yield at lower applied stresses and to dissipate more energy. Above these contents, the impact strength decreased because of agglomeration and decreasing interparticle spacing.

Some authors have applied dynamic viscosity (η^*) versus ω to calculate the power law index values and explain the shear thinning behavior of polymer nanocomposites in low- ω regions.^{16–18} For ω sweep data, the power law expression is written as follows:

$$\eta^* = k\omega^n \quad (1)$$

where k is a sample-specific preexponential factor, ω is the oscillation frequency in the frequency sweep

TABLE II
Power Law Indices

| Sample | n | R^2 |
|--------|------|-------|
| T2 | 0.43 | 0.999 |
| C2 | 0.56 | 0.999 |
| T5 | 0.55 | 0.999 |
| C5 | 0.61 | 0.999 |
| T15 | 0.36 | 0.999 |
| C15 | 0.68 | 0.999 |
| T30 | 0.50 | 0.998 |
| C30 | 0.61 | 0.999 |
| T60 | 0.55 | 0.998 |
| C60 | 0.65 | 0.998 |
| T100 | 0.54 | 0.999 |
| C100 | 0.64 | 0.999 |
| T200 | 0.60 | 0.998 |
| C200 | 0.79 | 0.999 |

test, and n is the shear thinning exponent. k and n can be directly determined from the logarithmic plot of η^* versus ω , as shown in eq. (2):

$$\log \eta^* = \log k + n \log \omega \quad (2)$$

The shear thinning exponent (n) is the slope of a straight line obtained by the plotting of $\log \eta^*$ versus $\log \omega$. n is a semiquantitative measure of the TiO₂ dispersion in the polymer phase. In this study, the power law model was applied to η^* curves of the samples in a low- ω region ($\omega = 0.17$ and 0.017 rad/s). Figure 5 illustrates the schematic shear thinning behavior of the T2, C2, T30, and C30 samples. Table II represents the power law indices of all of the samples. At the same ϕ_T , the pigment dispersion in the sample with the greater power law index was better. Obviously, at the same ϕ_T values (see Table II), the samples containing Cristal 134 had greater power law indices than the samples containing

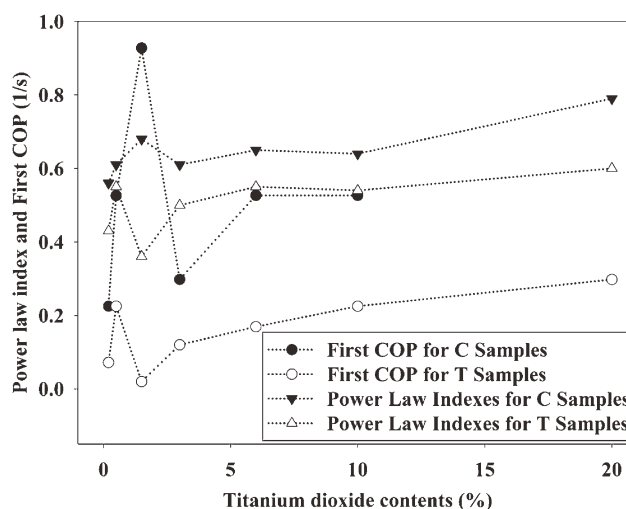


Figure 6 Variation curves of the first COPs and power law indices versus ϕ_T .

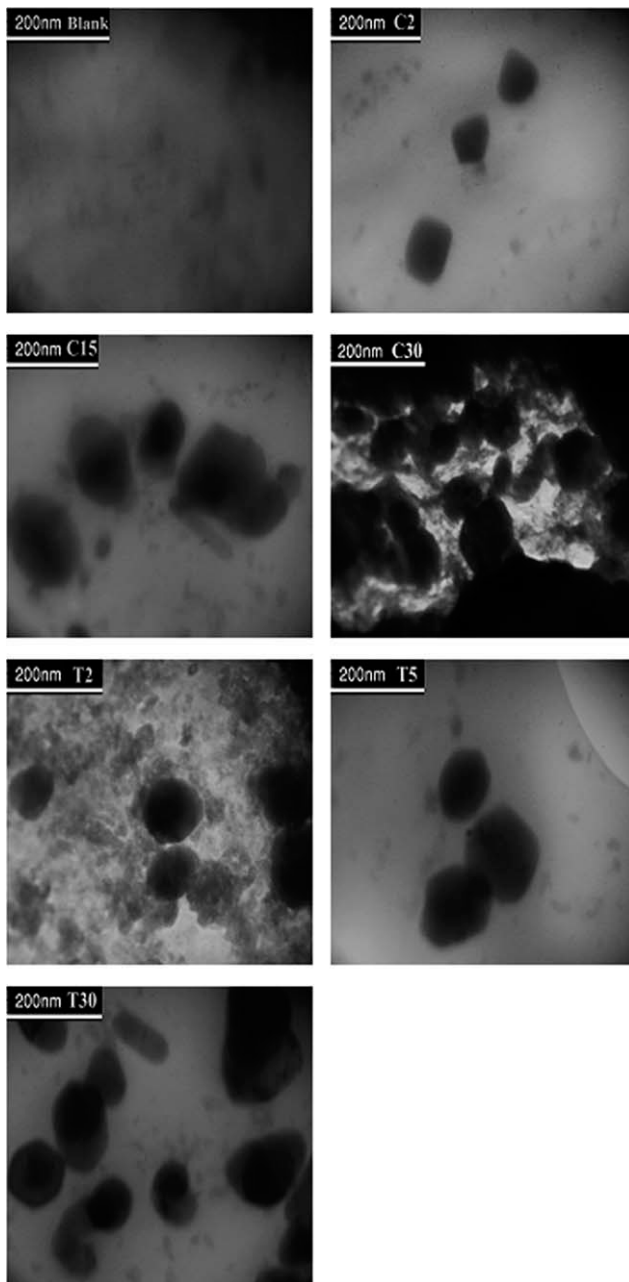


Figure 7 TEM micrographs of the TiO₂-pigmented ABS samples.

Tiona 188, and this showed that the TiO₂ dispersion at all contents of Cristal 134 was better in the matrix. In addition, a comparison between the maximum points in Figure 5 and the power law index versus ϕ_T plot showed that both trends were the same.

Figure 6 shows that the pigment agglomeration onsets were same in the two rheological methods (i.e., 1.5 and 0.5% for Cristal 134 and Tiona 188 pigmented samples, respectively). According to Figure 7, the TEM micrographs proved that the agglomerates of the Cristal 134 and Tiona 188 pigment particles were formed above 1.5 and 0.5%, respectively.

On the other hand, the particle size of dispersed BR particles could affect the rheological properties of ABS. The particle size of dispersed particles in suspensions can be changed by the presence of other particles in the mixing process, such as TiO₂ pigments. This phenomenon occurs because of the variation in thermodynamics and force fields during

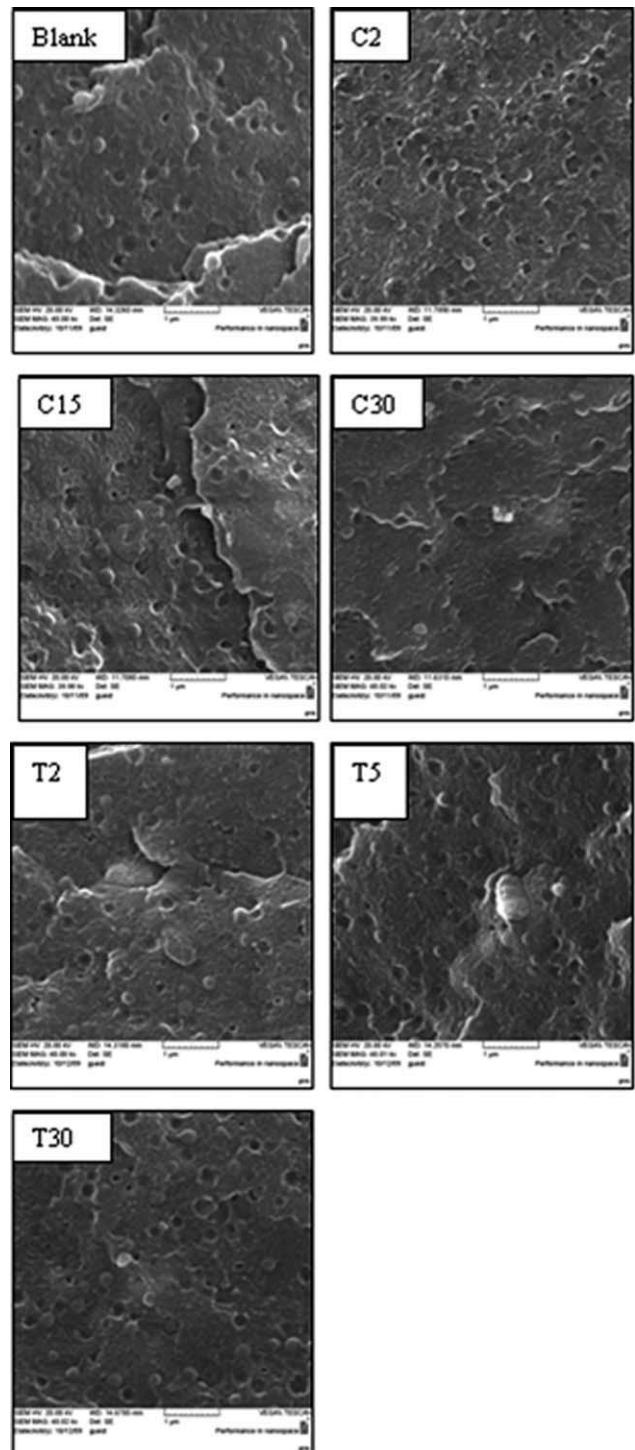


Figure 8 SEM micrographs of the surface of the broken ABS composites containing TiO₂ particles.

mixing and the relaxation processes of suspensions.¹⁹ However, in this study, the addition of TiO₂ particles almost had no effect on the BR particle size in the SAN media, and only a variation in the TiO₂ dispersion changed the rheological behavior of the complex fluid. This can be seen in the SEM images.

Figure 8 shows the SEM micrographs of the blank, C2, C15, C30, T2, T5, and T30 samples. The SEM micrograph of the blank sample shows that BR particles formed spherical particles and holes.²⁰ By viewing the SEM micrographs of the freeze-fractured surfaces of the samples, we could see that both TiO₂ pigments had no effect on the size of the BR particles. In each image, the size of the BR particles is between 150 and 300 nm. These values were confirmed by values obtained by Abbasi and Zeinali¹² for this general-purpose ABS.

Therefore, variations in the rheological properties and their plots occurred only because of the changes in the TiO₂ dispersions in the polymer media for the Tiona 188 and Cristal 134 samples.

CONCLUSIONS

Rheological measurements showed that the elasticity and first COPs increased with increases in the contents of the Tiona 188 and Cristal 134 pigments up to 0.5 and 1.5% in the matrix, respectively. Above these contents, with the addition of TiO₂, the first COPs dramatically decreased because of the agglomeration of the pigments and a decrease in their surface area. These variations were related to changes in the dispersion of TiO₂ particles in the matrix. This claim was confirmed by calculation of the power law indices (n parameter in the power law equation) of composite melts at low frequencies. In addition, SEM micrographs of the surfaces of the broken sam-

ples illustrated that the rubber particles size in SAN media showed no change with the addition of TiO₂; this indicated that changes in the rheological properties of the composites were due to changes in the TiO₂ particle dispersion.

References

1. Asiaban, S.; Taghinejad, S. F. *J Elast Plast* 2010, 42, 267.
2. Aoki, Y. *J SOCR Rheol Jpn* 2010, 7, 20.
3. Aoki, Y. *J Rheol* 1981, 25, 351.
4. Aoki, Y.; Nakayama, K. *J SOCR Rheol Jpn* 1981, 9, 39.
5. Aoki, Y.; Nakayama, K. *Polym J* 1982, 14, 951.
6. Bertin, M. P.; Marin, G.; Montfort, J. P. *Polym Eng Sci* 1995, 35, 1394.
7. Takahashi, M.; Li, L.; Masuda, T. *J Rheol* 1989, 33, 709.
8. Li, L.; Masuda, T.; Takahashi, M. *J Rheol* 1990, 34, 103.
9. Tang, C. Y.; Liang, J. Z. *Proceeding of the Ninth International Manufacturing Conference in China, The Hong Kong Polytechnic University, Hong Kong, 2000*; p 45.
10. Liang, J. Z. *Polym Int* 2002, 51, 1473.
11. Shang, S. W.; Williams, J. W.; Soderholm, K. M. *J Mater Sci* 1995, 34, 4323.
12. Abbasi, F.; Zeinali, A. Z. *Investigation of Rubber Particle Size, Distribution Size and Content on Physical and Mechanical Properties of ABS*, NPC R&T Co., Publishing Affair, Tehran, Iran, 2008.
13. Ferry, D. J. *Viscoelastic Properties of Polymers*; Wiley: New York, 1980.
14. Dealy, J. M.; Larson, R. G. *Structure and Rheology of Molten Polymers*; Hanser: Munich, 2006.
15. Charvat, R. A. *Coloring of Plastics: Fundamentals*; Wiley: Hoboken, NJ, 2004.
16. Durmus, A.; Kasgoz, A.; Macosko, C. W. *Polymer* 2007, 48, 4492.
17. Wagener, R.; Reisinger, T. J. G. *Polymer* 2003, 44, 7513.
18. Bellucci, F.; Camino, G.; Frache, A.; Ristori, V.; Sorrentino, L.; Iannace, S. *e-Polymer* 2006; paper no. 14.
19. Larson, R. G. *The Structure and Rheology of Complex Fluids*; Oxford University Press: New York, 1999.
20. Shenavar, A.; Abbasi, F. *J Appl Polym Sci* 2007, 105, 2236.